

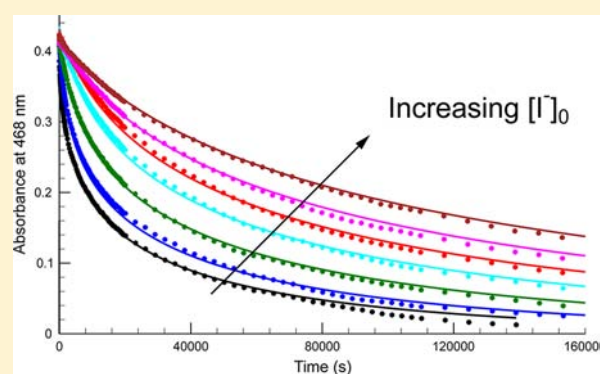
# General Pathway of Sulfur-Chain Breakage of Polythionates by Iodine Confirmed by the Kinetics and Mechanism of the Pentathionate–Iodine Reaction

Li Xu, György Csekő, Tamás Kégl, and Attila K. Horváth\*

Department of Inorganic Chemistry, University of Pécs, Ifjúság útja 6, H-7624 Hungary  
János Szentágotthai Research Center, Pécs, Ifjúság útja 34, H-7624 Hungary

## Supporting Information

**ABSTRACT:** The pentathionate–iodine reaction has been studied spectrophotometrically at  $T = 25.0 \pm 0.1$  °C and at an ionic strength of 0.5 M in both the absence and presence of an initially added iodide ion at the pH range of 3.95–5.15. It was found that the pH does not affect the rate of the reaction; however, the iodide ion produced by the reaction strongly inhibits the oxidation. Therefore, it acts as an autoinhibitor. The kinetic curves also support the fact that iodide inhibition cannot be explained by the formation of the unreactive triiodide ion, and  $S_5O_6I^-$  along with the iodide ion has to be involved in the initiating rapid equilibrium being shifted far to the left. Further reactions of  $S_5O_6I^-$ , including its hydrolysis and reaction with the iodide ion, lead to the overall stoichiometry represented by the following equation:  $S_5O_6^{2-} + 10I_2 + 14H_2O \rightarrow SSO_4^{2-} + 20I^- + 28H^+$ . A nine-step kinetic model with two fitted parameters is proposed and discussed, from which a rate equation has also been derived. A brief discussion about the general pathway of sulfur-chain breakage of polythionates supported by theoretical calculations has also been included.



## INTRODUCTION

The oxidation of thiosulfate by different oxidizing agents exhibits several exotic nonlinear dynamical phenomena, such as autocatalysis under batch conditions,<sup>1</sup> bistability and oscillations<sup>1,2</sup> or complex periodic and aperiodic (chaotic) behavior,<sup>3,4</sup> and multistationary states<sup>5</sup> in a continuously stirred tank reactor (CSTR), as well as the appearance of different kinds of reaction-diffusion patterns (chemical waves and chemical reaction fronts) in an unstirred system.<sup>6–9</sup> Besides the major product, sulfate, many sulfur-containing intermediates (mainly polythionates with a considerably long half-life) may be produced during the oxidation of thiosulfate.<sup>10,11</sup>

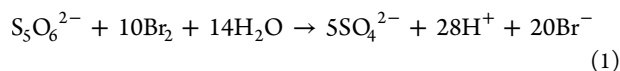
Compared to trithionate and tetrathionate, pentathionate is less stable in aqueous solution, especially at alkaline conditions,<sup>12</sup> but it is relatively stable at  $pH < 8.0$  and may therefore be a conceivable candidate as one of the sulfur-containing intermediates during the oxidation of thiosulfate. Recent researches have been shown that not only chemical but also electrochemical oxidation of thiosulfate leads to the formation of higher polythionates.<sup>13,14</sup> Moreover, the kinetic studies of hydrogen peroxide–thiosulfate,<sup>10</sup> chlorite–thiosulfate,<sup>11</sup> and hypochlorous acid–thiosulfate<sup>15</sup> systems have clearly demonstrated that pentathionate is formed in detectable amounts and may thus contribute to the appearance of a rich variety of kinetic phenomena<sup>4,6–9,16–18</sup> found experimentally in the oxidation reactions of thiosulfate. Compared to trithionate and tetrathio-

nate, however, significantly less information is available in the literature about the oxidation of pentathionate. We could track only a single study by Read et al.<sup>19</sup> that directly investigates the oxidation of pentathionate by the ferrate ion. Although little information is known about the redox reactions of pentathionate, we may expect similar kinetic behavior of polythionates because of their similar chemical structure. The reaction of pentathionate with iodine may be a good candidate to check this idea because, on the one hand, the reaction can easily be followed by UV–visible spectroscopy and, on the other hand, the kinetics of tetrathionate–iodine<sup>20,21</sup> as well as that of trithionate–iodine<sup>22</sup> reactions have already been available for comparison. The main outcome of these papers indicates that the oxidation of polythionates eventually leading to sulfate starts with an initiating equilibrium (a formal  $I^+$  transfer to the inner sulfur of the sulfur chain to produce  $S_xO_6I^-$ ) in which the iodide ion is also involved. Our aim in this paper is to obtain an additional support about the “nontriiodide”-based iodide inhibition, as well as to unravel the kinetics and mechanism of the analogous pentathionate–iodine reaction. As a result, it may also provide a better understanding and insight into the nature of the sulfur-chain-breaking reactions of pentathionate that may be helpful as a guide in unraveling more complex oxidation reactions of pentathionate.

Received: May 2, 2012

Published: June 28, 2012

**Materials and Instrumentation.** *Materials.* The potassium pentathionate was first prepared by the reaction of sodium thiosulfate with hydrochloric acid and arsenic oxide followed by ion exchange with a slurry of finely crystalline potassium acetate as described previously.<sup>23</sup> To confirm the purity of potassium pentathionate, Raman spectroscopy was carried out by a NXR Fourier transform Raman spectrometer. Its exact purity was checked by the following method. A known amount of potassium pentathionate was dissolved in pure distilled water followed by the addition of a bromine solution in excess. The reaction mixture was left to stand for at least 5 min, which was proven to be enough to oxidize pentathionate into sulfate completely. The excess of bromine was then removed by boiling the solution for a couple of minutes. The hydrogen ion, liberated by the oxidation of pentathionate by bromine according to the equation



was determined by titrating the sample against a standard sodium hydroxide solution. The purity of the solid potassium pentathionate sample was found to be better than 97.0% and checked prior to each experiment. No thiosulfate, sulfite, and elementary sulfur impurities could be detected up to 2–4 weeks. Because the composition of solid pentathionate<sup>23</sup> is  $\text{K}_2\text{S}_5\text{O}_6 \cdot \frac{1}{2}\text{H}_2\text{O}$ , this means that it may contain only a trace amount of sulfate or tetrathionate besides crystalline water. Once the purity of the solid sample was proven to be decreased because of the formation of elementary sulfur and other sulfur species, it was discarded and a new solid potassium pentathionate sample was prepared. All of the other chemicals (iodine, potassium iodide, acetic acid, sodium acetate, and sodium perchlorate) were of the highest purity commercially available and were used without further purification. The stock solutions were prepared from twice ion-exchanged and double-distilled water. The initial concentration of the iodine solution was determined by titration of the stock solutions with standardized thiosulfate and/or spectrophotometrically before each experiment.

The pH of the solutions was maintained between 3.95 and 5.15 by acetic acid/acetate buffer by taking the  $\text{pK}_a$  of acetic acid as 4.55.<sup>24</sup> The acetate concentration was always kept constant at 0.05 M, and the pH was adjusted by the necessary amount of acetic acid. The ionic strength was adjusted to be 0.5 M by adding the necessary amount of sodium perchlorate. The temperature of the reaction vessel was maintained at  $25.0 \pm 0.1$  °C. The initial concentrations of the reactants were varied in the ranges of 0.063–0.768, 0.0293–1.40, and 0–1.897 mM in the cases of iodine, pentathionate, and iodide, respectively.

**Methods and Instrumentation.** The reaction was followed by a Zeiss S600 diode-array spectrophotometer at the wavelength range of 400–800 nm without using the deuterium lamp of the photometer. The reaction has been carried out in a standard quartz cuvette equipped with a magnetic stirrer and a Teflon cap having 1 cm optical path. First, the buffer components, the reactant iodine, and iodide (if necessary) were delivered from a pipet. The spectrum of the solution was always recorded before injection of the pentathionate solution to determine the exact initial concentration of iodine. The reaction was started with the addition of the necessary amount of a pentathionate solution from a fast-delivery pipet.

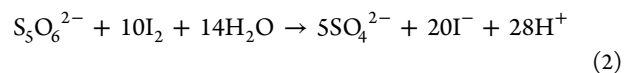
**Data Treatment.** In the visible range, only iodine and triiodide were found to absorb light; therefore, the isosbestic point of the iodine–triiodide system ( $\lambda = 468$  nm) was selected

for nonlinear parameter estimation by the *ZiTa* program package<sup>25</sup>. Altogether 23000 experimental points from 176 kinetic runs were used for simultaneous fitting. To obtain the kinetic model and the individual reaction rate coefficients, an absolute fitting procedure has been chosen to minimize the average deviation between measured and calculated concentrations. Our quantitative criterion for an acceptable fit was that the average deviation for the absolute fit approached 0.005 absorbance units, which is close to the experimentally achievable limit of error of the spectrophotometer.

**Computational Details of Theoretical Calculations.** For all of the calculations, the PBE0 functional was selected, i.e., the zero-parameter hybrid functional by Adamo and Barone<sup>26</sup> based on the generalized gradient approximation exchange and correlation functionals by Perdew, Burke, and Ernzerhof.<sup>27</sup> For all atoms, the def2-TZVPD triple- $\zeta$  basis set with polarization and diffuse basis functions<sup>28</sup> were employed. This model chemistry exhibited a reasonable agreement with the experimental geometrical parameters<sup>29</sup> for all species of the  $\text{S}_x\text{O}_6^{2-}$  type ( $x = 3-5$ ). Optimized geometries were identified by the absence of negative eigenvalues in the vibrational frequency analysis. Geometry optimizations were completed with solvent effects taken into account by employing the polarizable continuum model methodology<sup>30</sup> with dielectric constant  $\epsilon = 78.355$  for water. For all of the calculations, the Firefly 7.1.G quantum chemical package<sup>31</sup> was used. Natural bond orbital (NBO) analyses<sup>32</sup> have been performed by the module NBO 5.G implemented in Firefly.

## ■ RESULT

**Stoichiometry.** The stoichiometry of the reaction was established by visible spectroscopy from the end of the kinetic measurements in an excess of iodine. The calculation indicated that the ratio of iodine and pentathionate is 10 and the only sulfur-containing product of the reaction is the sulfate ion. Therefore, the stoichiometry of this reaction can be expressed as follows:



**Individual Curve-Fitting Method.** Survey of the experimental curves in the pentathionate–iodine reaction reveals two important characteristics of this system. On the one hand, the decay of iodine is independent of the pH within the pH range used in the experiments, as seen in Figure 1. The same phenomenon has also been reported in the tetrathionate–iodine<sup>20,21</sup> and trithionate–iodine<sup>22</sup> systems, meaning that this feature is a general phenomenon of the polythionate–iodine reactions. On the other hand, Figure 2 describes the effect of the initially added iodide ion on the consumption of the total amount of iodine. It clearly demonstrates that an increase of the initial iodide concentration significantly inhibits the pentathionate–iodine reaction. Therefore, the iodide ion acts as an autoinhibitor of the system because its concentration monotonously increases during the course of the reaction. To account for all of these observations, our first effort to evaluate the kinetic curves individually was, therefore, based on the following apparent rate equation:

$$-\frac{1}{10} \frac{dT_{\text{I}_2}}{dt} = k_{\text{app}} \frac{[\text{S}_5\text{O}_6^{2-}]T_{\text{I}_2}}{[\text{I}^-]} \quad (3)$$

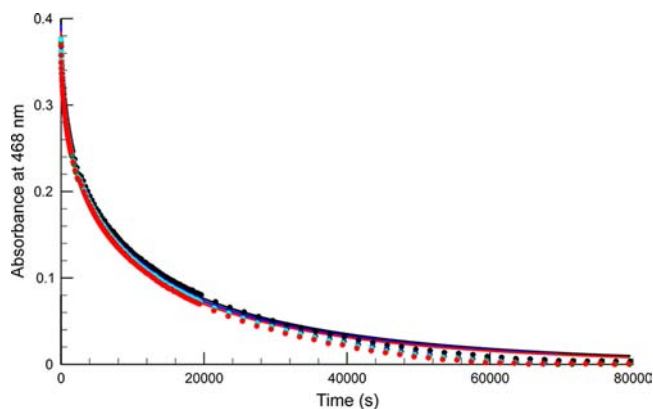


**Figure 1.** Measured (dots) and calculated (solid lines) absorbance–time curves at  $[S_5O_6^{2-}]_0 = 0.201$  mM and  $[I_2]_0 = 0.511$  mM at different pH values in the absence of the initially added iodide ion. pH = 3.95 (black), 4.25 (blue), 4.55 (green), 4.85 (cyan), and 5.15 (red).

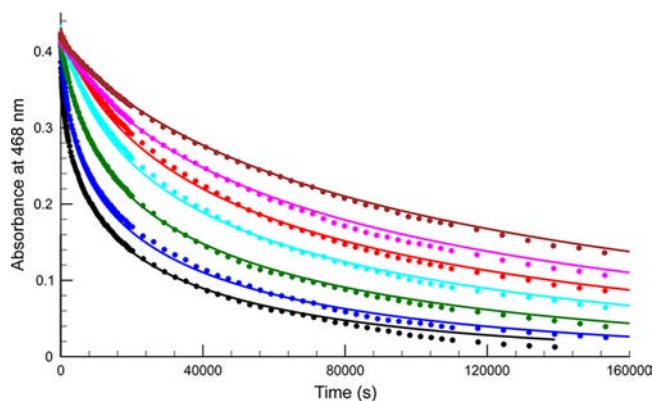


**Figure 2.** Measured (dots) and calculated (solid lines) absorbance–time curves at  $[S_5O_6^{2-}]_0 = 0.11$  mM,  $[I_2]_0 = 0.56$  mM, and pH = 4.55 in the presence of the initially added iodide ion.  $[I^-]_0/\text{mM} = 0.0$  (black), 0.101 (blue), 0.399 (green), 0.699 (cyan), 0.998 (red), 1.397 (magenta), and 1.796 (brown).

where  $T_{I_2} = [I_2] + [I_3^-]$ . The surprising results of our calculation is that eq 3 is able to fit all of the 176 kinetic curves with  $k_{app}$  equal to  $(3.15 \pm 0.50) \times 10^{-5} \text{ s}^{-1}$  within an acceptable error, although we also noticed that  $k_{app}$  slightly decreases as the initial concentration of iodide increases. This feature is illustrated in Table 1. Later we shall see that this feature can easily be explained by the proposed model.

**Proposed Kinetic Model.** Because the overall reaction produces a relatively huge amount of proton (see eq 2), the protonation and deprotonation processes of the buffer components would seem to be necessary to follow the slight change of the pH during the course of the reaction:



However, as shown above, the pH does not affect the reaction; therefore, this equilibrium was only taken into consideration for the sake of completeness. Our first effort was to describe all of the 176 kinetic curves simultaneously based on eq 2, which was augmented by the well-known triiodide formation equilibrium:



In this model, the iodide inhibition was taken into consideration simply by the formation of the kinetically inactive triiodide ion and the rate equation of eq 2 was considered to be an overall

**Table 1.** Apparent Rate Coefficients of Representative Examples Determined by the Individual Curve-Fitting Method

$[S_5O_6^{2-}]_0/\text{mM}$	$[I_2]_0/\text{mM}$	$[I^-]_0/\text{mM}$	pH	$k_{app} \times 10^5 \text{ s}^{-1}$
0.03	0.455	0	3.95	3.73
0.06	0.43	0	3.95	3.48
0.121	0.445	0	3.95	3.17
0.251	0.45	0	3.95	3.15
0.5	0.45	0	3.95	3.23
0.8	0.41	0	3.95	3.25
1.401	0.42	0	3.95	3.13
0.05	0.064	0	4.85	3.78
0.05	0.096	0	4.85	3.67
0.05	0.18	0	4.85	3.33
0.05	0.245	0	4.85	3.38
0.05	0.355	0	4.85	3.25
0.05	0.509	0	4.85	3.37
0.05	0.732	0	4.85	3.76
0.061	0.533	0	3.95	3.35
0.061	0.543	0	4.25	3.20
0.061	0.533	0	4.55	3.17
0.061	0.538	0	4.85	3.09
0.061	0.533	0	5.15	3.25
0.489	0.520	0	4.55	3.02
0.489	0.520	0.100	4.55	2.66
0.489	0.520	0.499	4.55	2.54
0.489	0.515	0.999	4.55	2.25
0.489	0.512	1.300	4.55	2.14
0.489	0.515	1.600	4.55	1.95
0.489	0.520	1.897	4.55	1.83

second-order reaction, having the formal kinetic order of both reactants as 1. This kinetic model fits all of the data with an unacceptably high average deviation of 0.046 absorbance units. We therefore concluded that inhibition of the iodide ion cannot be taken into account only by the formation of the triiodide ion. On the basis of the remarkable resemblance of the kinetic behavior of the polythionate–iodine reactions,<sup>20–22</sup> we suggest the kinetic models R1–R9 similar to the reactions mentioned above:

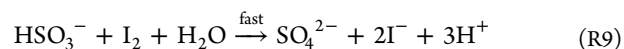
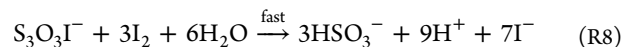
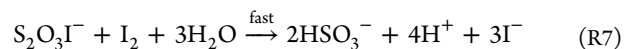
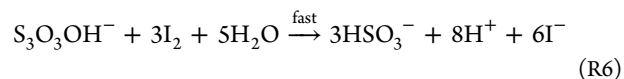
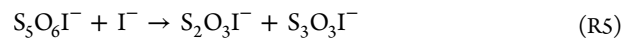
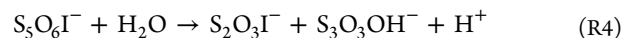
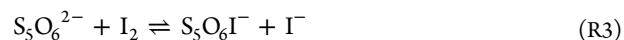
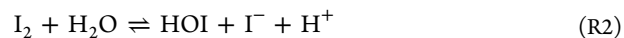
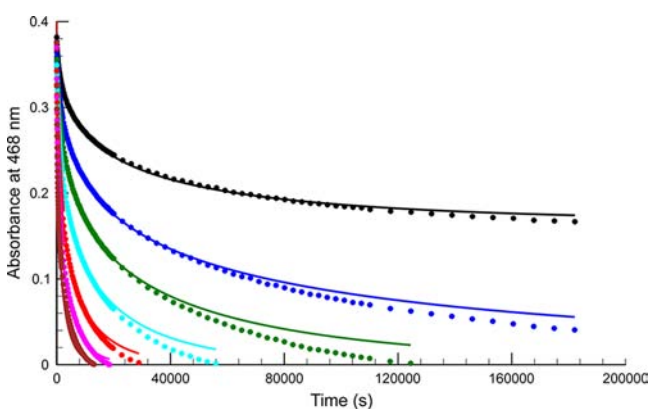


Table 2 contains the parameter set determined by the simultaneous evaluation of the kinetic curves, and the results are illustrated in Figures 1–4. (Supporting Information is also available to show the results of the fits for all of the 176 measured kinetic curves.) By the proposed kinetics, we were able to

**Table 2. Fitted and Fixed Rate Coefficients of the Proposed Kinetic Model<sup>a</sup>**

step	rate equation	parameter
R1	$k_{R1}[I_2][I^-]$	$5.7 \times 10^9 \text{ M}^{-1} \text{ s}^{-1}$
	$k_{-R1}[I_3^-]$	$8.5 \times 10^6 \text{ s}^{-1}$
R2	$k_{R2}[I_2]$	$5.52 \times 10^{-2} \text{ s}^{-1}$
	$k_{-R2}[\text{HOI}][\text{H}^+][I^-]$	$1.023 \times 10^{11} \text{ M}^{-2} \text{ s}^{-1}$
	$k'_{R2}[I_2]/[\text{H}^+]$	$1.98 \times 10^{-3} \text{ M s}^{-1}$
	$k'_{-R2}[\text{HOI}][I^-]$	$3.67 \times 10^9 \text{ M}^{-1} \text{ s}^{-1}$
R3	$k_{R3}[\text{S}_5\text{O}_6^{2-}][I_2]$	$10^1 \text{ M}^{-1} \text{ s}^{-1}$
	$k_{-R3}[\text{S}_5\text{O}_6\text{I}^-][I^-]$	$10^6 \text{ M}^{-1} \text{ s}^{-1}$
R4	$k_{R4}[\text{S}_5\text{O}_6\text{I}^-]$	$3.29 \pm 0.06 \text{ s}^{-1}$
R5	$k_{R5}[\text{S}_5\text{O}_6^{2-}][I^-]$	$310 \pm 66 \text{ M}^{-1} \text{ s}^{-1}$
R6	$k_{R6}[\text{S}_3\text{O}_3\text{OH}^-][I_2]$	$>10^2 \text{ M}^{-1} \text{ s}^{-1}$
R7	$k_{R7}[\text{S}_2\text{O}_3\text{I}^-][I_2]$	$>10^2 \text{ M}^{-1} \text{ s}^{-1}$
R8	$k_{R8}[\text{S}_3\text{O}_3\text{I}^-][I_2]$	$>10^3 \text{ M}^{-1} \text{ s}^{-1}$
R9	$k_{R9}[\text{HSO}_3^-][I_2]$	$3.1 \times 10^9 \text{ M}^{-1} \text{ s}^{-1}$

<sup>a</sup>No error indicates that the value in question was fixed during the fitting procedure.



**Figure 3.** Measured (dots) and calculated (solid lines) absorbance–time curves at  $[I_2]_0 = 0.51 \text{ mM}$  and  $\text{pH} = 4.55$  in the absence of the initially added iodide ion.  $[\text{S}_5\text{O}_6^{2-}]_0/\text{mM} = 0.03$  (black),  $0.06$  (blue),  $0.101$  (green),  $0.201$  (cyan),  $0.400$  (red),  $0.800$  (magenta), and  $1.401$  (brown).

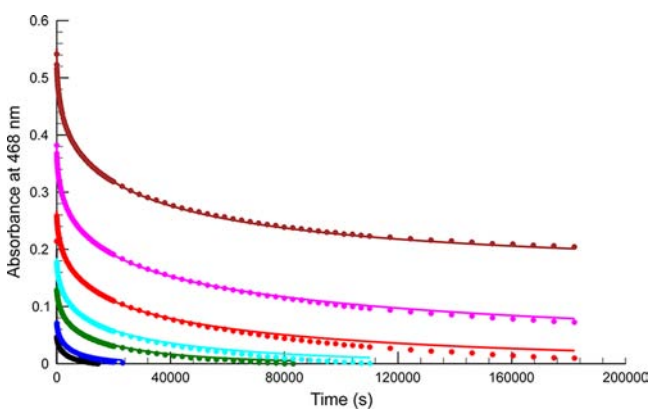


**Figure 4.** Measured (dots) and calculated (solid lines) absorbance–time curves at  $[\text{S}_5\text{O}_6^{2-}]_0 = 0.05 \text{ mM}$  and  $\text{pH} = 4.85$  in the absence of the initially added iodide ion.  $[I_2]_0/\text{mM} = 0.064$  (black),  $0.096$  (blue),  $0.18$  (green),  $0.245$  (cyan),  $0.355$  (red),  $0.509$  (magenta), and  $0.732$  (brown).

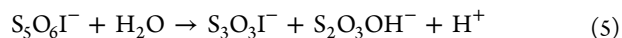
describe all of the 176 kinetic curves by 0.0048 absorbance unit average deviation, suggesting the plausibility of our kinetic model.

**Discussion.** Step R1 is the well-known fast equilibrium of the formation of the triiodide ion studied by several authors.<sup>33,34</sup> The rate coefficients of the forward and reverse reactions were set to  $k_{R1} = 5.7 \times 10^9 \text{ M}^{-1} \text{ s}^{-1}$  and  $k_{-R1} = 8.5 \times 10^6 \text{ s}^{-1}$  to give  $\log \beta_{I_3^-} = 2.83$ , where  $\beta_{I_3^-}$  is the formation constant of the triiodide ion.<sup>24</sup>

Step R2 is the hydrolytic equilibrium of iodine in an aqueous solution. The rate coefficients of the forward and reverse reactions including the hydroxide-driven pathway were determined previously; therefore, we used these values as fixed ones throughout the whole fitting procedure.<sup>35–37</sup>

Step R3 is a rapid initiating equilibrium between the reactants, producing  $\text{S}_5\text{O}_6\text{I}^-$  and the iodide ion. Later we shall see that the attack of the iodine molecule is likely to occur on the  $\beta$  (or  $\beta'$ )-sulfur of pentathionate. Our calculation has provided only a higher limit for  $K_{R3} = k_{R3}/k_{-R3} = 0.01$ ; any value lower than that leads to the same average deviation, meaning that this equilibrium is shifted far to the left. To provide a low steady-state concentration for the species  $\text{S}_5\text{O}_6\text{I}^-$ , we have set  $k_{R3} = 10 \text{ M}^{-1} \text{ s}^{-1}$  and  $k_{-R3} = 10^6 \text{ M}^{-1} \text{ s}^{-1}$  to provide  $K_{R3} = 10^{-5}$  during the calculation process.

Step R4 is one of the possible pathways of  $\text{S}_5\text{O}_6\text{I}^-$  to produce additional sulfur-containing short-lived intermediates via the breakup of the sulfur chain. The solvent water molecule probably attacks the  $\gamma$ -sulfur of the sulfur chain (an attack on  $\beta'$ -sulfur cannot be ruled out entirely), resulting in  $\text{S}_2\text{O}_3\text{I}^-$  and  $\text{S}_3\text{O}_3\text{OH}^-$ . Because both species are short-lived intermediates, our kinetic measurements do not provide a solid basis to distinguish between step R4 and the following reaction:



One should keep in mind that iodine in  $\text{S}_3\text{O}_3\text{I}^-$  is placed on the inner sulfur and not on the terminal one to be in agreement that iodine attacks the  $\beta$ -sulfur of the sulfur chain. If further reaction of  $\text{S}_2\text{O}_3\text{OH}^-$  with iodine is considered to be a rapid reaction resulting in the formation of hydrogen sulfite as well, step R4 can easily be replaced by eq 5 kinetically. However, as we show later, the attack of the oxygen atom of the solvent molecule most likely takes place on the  $\gamma$ -sulfur of  $\text{S}_5\text{O}_6\text{I}^-$ ; therefore, we are rather inclined to keep step R4 in the final model. If  $K_{R3} = 10^{-5}$  is used to provide a low steady-state concentration for  $\text{S}_5\text{O}_6\text{I}^-$ , we could calculate  $k_{R4} = 3.29 \pm 0.06 \text{ s}^{-1}$ . Our fitting also indicated that  $k_{R4}$  and  $K_{R3}$  cannot be determined independently because of the strong correlation between these kinetic parameters; only their product could be calculated. Later we shall see that this fact can conveniently be explained by the overall rate equation obtained from the proposed kinetic model.

Step R5 is the other important conversion reaction of  $\text{S}_5\text{O}_6\text{I}^-$  in which the iodide ion probably attacks one of the inner sulfurs of the sulfur chain, resulting in the breakup of the sulfur–sulfur bond as well. Such a reaction of the intermediate  $\text{S}_5\text{O}_6\text{I}^-$  with the iodide ion was already proposed in the tetrathionate–iodine reaction<sup>21</sup> and turns out to be necessary to describe adequately the polythionate–iodine reactions. It was found that the individual rate coefficient of this reaction cannot be determined as well because of the strong correlation between the rate coefficients of  $k_{R3}$ ,  $k_{-R3}$ , and  $k_{R5}$ ; only the product of  $K_{R3}$  and  $k_{R5}$  can be calculated unambiguously. As a result, if  $K_{R3} = 10^{-5}$  was considered in the calculation process, we obtained  $k_{R5} = 310 \pm 66 \text{ M}^{-1} \text{ s}^{-1}$ .

Steps R6–R8 are fast processes in which the short-lived intermediates  $S_3O_3OH^-$ ,  $S_2O_3I^-$ , and  $S_3O_3I^-$  are oxidized by iodine, resulting in hydrogen sulfite and the iodide ion. All of these reactions were found to be rapid processes, and only the lower limits of  $k_{R6}$ ,  $k_{R7}$ , and  $k_{R8}$  (indicated in Table 2) could be determined from our measurements.

Step R9 is the rapid, essentially diffusion-controlled, reaction of hydrogen sulfite and iodine studied thoroughly by Yiin and Margerum.<sup>38</sup> The  $k_{R9} = 3.1 \times 10^9 \text{ M}^{-1} \text{ s}^{-1}$  value was determined in their work for its rate coefficient, and we fixed it throughout the whole calculation process.

**Formal Kinetics.** Because no intermediates were found in a detectable amount during the course of the reaction, a rate equation can easily be deduced from the proposed model. Considering that

$$-\frac{1}{10} \frac{dT_{I_2}}{dt} = -\frac{d[S_5O_6^{2-}]}{dt} = k_{R3}[S_5O_6^{2-}][I_2] - k_{-R3}[S_5O_6I^-][I^-] \quad (6)$$

and applying a steady-state approximation for species  $S_5O_6I^-$  yield

$$[S_5O_6I^-] = \frac{k_{R3}[S_5O_6^{2-}][I_2]}{k_{R4} + (k_{-R3} + k_{R5})[I^-]} \quad (7)$$

Upon substitution of eq 7 into eq 6, followed by some algebraic manipulation, we arrive at

$$-\frac{1}{10} \frac{dT_{I_2}}{dt} = -\frac{d[S_5O_6^{2-}]}{dt} = [S_5O_6^{2-}]T_{I_2}(k_{R3}k_{R4} + k_{R3}k_{R5}[I^-]) / \{k_{R4} + (k_{-R3} + k_{R5} + k_{R4}K_{R1})[I^-] + K_{R1}(k_{-R3} + k_{R5})[I^-]^2\} \quad (8)$$

where  $K_{R1}$  is the formation constant of triiodide. Taking into account that the  $k_{-R3} \gg k_{R5} + k_{R4}K_{R1}$  inequality is fulfilled and  $k_{-R3}[I^-] \gg k_{R4}$  holds apart from the very beginning stage of the reaction, the following equation is obtained:

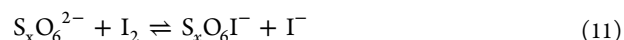
$$-\frac{1}{10} \frac{dT_{I_2}}{dt} = \frac{K_{R3}k_{R4} + K_{R3}k_{R5}[I^-]}{1 + K_{R1}[I^-]} \frac{[S_5O_6^{2-}]T_{I_2}}{[I^-]} \quad (9)$$

Comparing eq 9 with eq 3, one can easily see that  $k_{app}$  slightly depends on the actual iodide concentration.

$$k_{app} = \frac{K_{R3}k_{R4} + K_{R3}k_{R5}[I^-]}{1 + K_{R1}[I^-]} \quad (10)$$

Substituting the rate coefficients determined here at low initial iodide concentration, we can calculate  $3.15 \times 10^{-5} \text{ s}^{-1}$  for  $k_{app}$ , while at high initial iodide concentration,  $k_{app} = 0.6 \times 10^{-5} \text{ s}^{-1}$  can be obtained. Comparing these values with the experimentally determined  $k_{app}$  values at different initial conditions (see Table 1), we find that the results strongly support our proposed kinetic model as well. This equation also helps to understand why only the products of  $K_{R3}k_{R4}$  and  $K_{R3}k_{R5}$  can be calculated from our experiments.

**General Pathway of the Sulfur-Chain Breakage of Polythionates.** Previous studies of trithionate<sup>22</sup> and tetrathionate<sup>20,21</sup> oxidation by iodine as well as our present results suggest the fact that the sulfur-chain breakage of polythionates starts generally with the same equilibrium:



where  $x = 3-5$ . This equilibrium is shifted far to the left and established rapidly compared to the time scale of the reaction in question. Should these reactions start with formal  $I^+$ , the inhibitory effect of the iodide can easily be explained by eq 11. As shown previously,<sup>20-22</sup> the formation of the kinetically inactive triiodide formation in itself is not able to explain the inhibitory effect of the iodide ion. From these studies, it was also enlightened that the following rate equation describes well the kinetic curves of all of the polythionates–iodine reactions:

$$v = k_x \frac{[S_xO_6^{2-}]T_{I_2}}{[I^-]} \quad (12)$$

where  $10^5 k_x = 82.7, 4.1, \text{ and } 3.15 \text{ s}^{-1}$  in the case of trithionate, tetrathionate, and pentathionate, respectively. From these values, one can easily calculate that the half-lives of the corresponding trithionate–iodine, tetrathionate–iodine, and pentathionate–iodine reactions are 840, 16900, and 22000 s, respectively. In other words, this means that a longer sulfur chain of polythionates corresponds to a more sluggish reaction toward iodine. It raises an important question about the attack of iodine on polythionates at a molecular level. Figure 5 indicates the

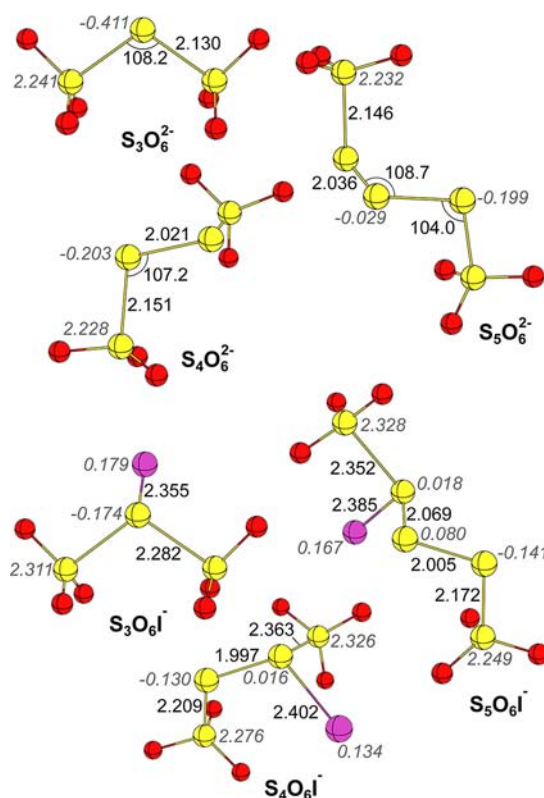


**Figure 5.** Molecular structures of polythionates and  $S_xO_6I^-$  species calculated at the PBE0/TZVPD level of theory. Bond distances are given in angstroms and bond angles in degrees. Natural charges are written in italics.

calculated structures of polythionates and  $S_xO_6I^-$  species. It is seen that among the polythionates the  $\beta$ -sulfur of trithionate has the most negative partial charge ( $-0.411$ ). Compared to this, the partial charge of the  $\beta$  (and  $\beta'$ )-sulfur atom decreases to  $-0.203$  in the case of tetrathionate, but a further increase of the sulfur chain results in a minor change only (to  $-0.199$ ) for the partial

charge of  $\beta$ - and  $\beta'$ -sulfur atoms in the case of pentathionate. Because the  $\beta$  (and  $\beta'$ )-sulfur of the polythionate sulfur chain is negatively charged, this site is a possible candidate to be attacked by iodine and, furthermore, supports a formal  $I^+$  transfer to the  $\beta$ -sulfur of the polythionate chain. Moreover, the increase of the partial charge of the  $\beta$ -sulfur of  $S_xO_6I^-$  compared to those of the corresponding polythionates (0.237, 0.219, and 0.217 electrons for the trithionate, tetrathionate, and pentathionate, respectively) may also explain why the trithionate–iodine reaction is faster by more than 1 order of magnitude compared to the tetrathionate–iodine and pentathionate–iodine reactions and why there is not much difference between the rates of the tetrathionate–iodine and pentathionate–iodine reactions. The central kinetic role of the  $\beta$  (and  $\beta'$ )-sulfur of the sulfur chain is also supported by the well-known catalytic effect of thiosulfate on the rearrangement of tetrathionate.<sup>39</sup> Once  $S_xO_6I^-$  forms, one may easily see that the length of the bond between the  $\alpha$ - and  $\beta$ -sulfur atoms increases in each polythionate in the range of 0.152–0.212 Å, facilitating an attack of the solvent molecule to finally break up the sulfur chain. The fate of  $S_xO_6I^-$ , however, differs in the case of trithionate compared to those of the higher polythionates. In the former case,  $S_3O_6I^-$  has two different routes for sulfur-chain breakup: hydrolysis and the reaction of iodine.<sup>22</sup> In the other cases, however, besides the hydrolysis, the attack of the iodide ion is also a possible route for  $S_xO_6I^-$  to be converted. The lack of attack of the iodide ion on  $S_3O_6I^-$  may easily be explained by the lack of a sterically not hidden positively charged sulfur atom of the molecule. Our present study of the pentathionate–iodine reaction reveals that  $S_5O_6I^-$  can also be attacked by the iodide ion to break up the sulfur chain. As can be seen, the  $\beta$ - and  $\gamma$ -sulfur atoms are partially positively charged parts of the molecule that can be attacked by the electron-rich iodide ion. This further attack (which probably takes place on the  $\gamma$ -sulfur because of its slightly more positive partial charge) increases the length of the  $\beta$ -sulfur– $\gamma$ -sulfur bond, resulting in its immediate breakup. Once the sulfur chain breaks up, the following rapidly oxidizing processes eventually lead to the formation of sulfate.

## CONCLUSION

The work presented here is the first trial to describe the kinetics and mechanism of the pentathionate–iodine reaction. As shown, it is demonstrated that the reaction is independent of the pH within the pH range studied and exhibits strong iodide autoinhibition that emerges from the initiating equilibrium between the reactants, resulting in the formation of  $S_5O_6I^-$  and the iodide ion. As pointed out throughout a comparison of the studies of trithionate–iodine and tetrathionate–iodine as well, this phenomenon seems to be general among the sulfur-chain-breaking reaction of polythionate with the mild oxidizing agent iodine. We also hope that the present study will inspire some further theoretical investigations to obtain deeper insight into the nature of sulfur-chain-breaking reactions of polythionates. Understanding these reactions more thoroughly may contribute to better descriptions of nonlinear exotic phenomena in which polythionates, mainly tetrathionate, are seriously involved.

## ASSOCIATED CONTENT

### Supporting Information

Table containing the conditions of each kinetic run and figures containing the measured and fitted data. This material is available free of charge via the Internet at <http://pubs.acs.org>.

## AUTHOR INFORMATION

### Corresponding Author

\*E-mail: [horvatha@gamma.ttk.pte.hu](mailto:horvatha@gamma.ttk.pte.hu).

### Notes

The authors declare no competing financial interest.

## ACKNOWLEDGMENTS

This work was supported by the Hungarian Research Fund (Grant CK78553). The authors are grateful to Dr. Andrea Petz for her helpful assistance in the Raman measurements. L.X. is thankful for financial support from the China Scholarship Council.

## REFERENCES

- (1) Orbán, M.; Kepper, P. D.; Epstein, I. R. *J. Phys. Chem.* **1982**, *86*, 431–433.
- (2) Rábai, G.; Beck, M. T.; Kustin, K.; Epstein, I. R. *J. Phys. Chem.* **1989**, *93*, 2853–2858.
- (3) Orbán, M.; Epstein, I. R. *J. Phys. Chem.* **1982**, *86*, 3907–3910.
- (4) Maselko, J.; Epstein, I. R. *J. Chem. Phys.* **1984**, *80*, 3175–3178.
- (5) Orbán, M.; Epstein, I. R. *J. Am. Chem. Soc.* **1987**, *109*, 101–106.
- (6) Nagypál, I.; Bazsa, G.; Epstein, I. R. *J. Am. Chem. Soc.* **1986**, *108*, 3635–3640.
- (7) Szivovics, L.; Nagypál, I.; Bárdi, I. *Int. J. Chem. Kinet.* **1991**, *23*, 99–101.
- (8) Zhitovniko, V. V.; Koptyug, I. V.; Sagdeev, R. Z. *J. Phys. Chem. A* **2007**, *111*, 4122–4124.
- (9) Koptyug, I. V.; Zhitovniko, V. V.; Sagdeev, R. Z. *J. Phys. Chem. B* **2008**, *112*, 1170–1176.
- (10) Lu, Y.; Gao, Q.; Xu, L.; Zhao, Y.; Epstein, I. R. *Inorg. Chem.* **2010**, *49*, 6026–6034.
- (11) Xu, L.; Horváth, A. K.; Hu, Y.; Ji, C.; Zhao, Y.; Gao, Q. *J. Phys. Chem. A* **2011**, *115*, 1853–1860.
- (12) (a) Christiansen, J. A.; Drost-Hansen, W.; Nielsen, A. *Acta Chem. Scand.* **1952**, *6*, 333–340. (b) Goehring, M.; Heibing, W.; Appel, I. Z. *Anorg. Chem.* **1947**, *254*, 185–200. (c) Wagner, H.; Schreier, H. *Phosphorus Sulfur Relat. Elem.* **1978**, *4*, 281–284. (d) Wagner, H.; Schreier, H. *Phosphorus Sulfur Relat. Elem.* **1978**, *4*, 285–286. (e) Pan, C. W.; Wang, W.; Horváth, A. K.; Xie, J.; Lu, Y.; Wang, Z.; Ji, C.; Gao, Q. *Inorg. Chem.* **2011**, *50*, 9670–9677.
- (13) Du, Z.; Gao, Q.; Feng, J.; Lu, Y.; Wang, J. *J. Phys. Chem. B* **2006**, *110*, 26098–26104.
- (14) Jeffrey, M. I.; Brunt, S. D. *Hydrometallurgy* **2007**, *89*, 52–60.
- (15) Varga, D.; Horváth, A. K.; Nagypál, I. *J. Phys. Chem. B* **2006**, *110*, 2467–2470.
- (16) Yuan, L.; Gao, Q.; Zhao, Y.; Tang, X.; Epstein, I. R. *J. Phys. Chem. A* **2010**, *114*, 7014–7020.
- (17) Kurin-Csörgei, K.; Orbán, M.; Rábai, G.; Epstein, I. *J. Chem. Soc., Faraday Trans.* **1996**, *92*, 2851–2855.
- (18) Rábai, G.; Hanazaki, I. *J. Phys. Chem. A* **1999**, *103*, 7268–7273.
- (19) Read, J. F.; Bewick, S. A.; Donaher, S. C.; Ealman, M. D.; Oakey, J.; Schaubel, C.; Tam, N. C.; Theriault, A.; Watson, K. J. *Inorg. React. Mech.* **2005**, *5*, 281–304.
- (20) Kerek, A.; Horváth, A. K. *J. Phys. Chem. A* **2007**, *111*, 4235–4241.
- (21) Awtrey, A. D.; Connick, R. E. *J. Am. Chem. Soc.* **1951**, *73*, 4546–4549.
- (22) Csekő, G.; Horváth, A. K. *J. Phys. Chem. A* **2010**, *114*, 6521–6526.
- (23) Kelly, D. P.; Wood, A. P. *Methods Enzymol.* **1994**, *243*, 475–501.
- (24) *IUPAC Stability Constant Database*; Royal Society of Chemistry: London, 1992–1997.
- (25) Peintler, G. *ZiTa, version 5.0; a comprehensive program package for fitting parameters of chemical reaction mechanism*; Attila József University: Szeged, Hungary, 1989–1998.
- (26) Adamo, C.; Barone, V. *J. Chem. Phys.* **1999**, *110*, 6158–6170.
- (27) Perdew, J. P.; Burke, K.; Ernzerhof, M. *Phys. Rev. Lett.* **1996**, *77*, 3865–3868.

- (28) Rappoport, D.; Furche, F. *J. Chem. Phys.* **2010**, *133*, 134105–134115.
- (29) Greenwood, N. N.; Earnshaw, A. *Chemistry of the Elements*, 2nd ed.; Butterworth-Heinemann: New York, 1997.
- (30) Tomasi, J.; Persico, M. *Chem. Rev.* **1994**, *94*, 2027–2094.
- (31) Granovsky, A. A. *Firefly*, version 7.1.G, <http://classic.chem.msu.su/gran/firefly/index.html>.
- (32) Reed, A. E.; Curtiss, L. A.; Weinhold, F. *Chem. Rev.* **1988**, *88*, 899–926.
- (33) Turner, D. H.; Flynn, G. W.; Sutin, N.; Beitz, J. V. *J. Am. Chem. Soc.* **1972**, *94*, 1554–1559.
- (34) Ruasse, M.; Aubard, J.; Galland, B.; Adenier, A. *J. Phys. Chem.* **1986**, *90*, 4382–4388.
- (35) Eigen, M.; Kustin, K. *J. Am. Chem. Soc.* **1962**, *84*, 1355–1361.
- (36) Lengyel, I.; Epstein, I. R.; Kustin, K. *Inorg. Chem.* **1993**, *32*, 5880–5882.
- (37) Lengyel, I.; Li, J.; Kustin, K.; Epstein, I. R. *J. Am. Chem. Soc.* **1996**, *118*, 3708–3719.
- (38) Yiin, B. S.; Margerum, D. W. *Inorg. Chem.* **1990**, *29*, 1559–1564.
- (39) Fava, A.; Bresadola, S. *J. Am. Chem. Soc.* **1955**, *77*, 5792–5794.